Molecular Crystals and Liquid Crystals
Publication details, including instructions for authors and subscription information:
http://www.tandfonline.com/loi/gmcl16

Harmonic Dynamics of Anthracene Crystal

T. A. Krivenko [a], V. A. Dementjev [b], E. L. Bokhenkov [a], A. I. Kolesnikov [a] & E. F. Sheka [a]

[a] Institute of Solid State Physics of the Academy of Sciences of the USSR, 142432, Chernogolovka, USSR

[b] Timiryazev Agricultural Academy, 125008, Moscow, USSR

Version of record first published: 20 Apr 2011.

To cite this article: T. A. Krivenko , V. A. Dementjev , E. L. Bokhenkov , A. I. Kolesnikov & E. F. Sheka (1984): Harmonic Dynamics of Anthracene Crystal, Molecular Crystals and Liquid Crystals, 104:3-4, 207-230

To link to this article: http://dx.doi.org/10.1080/00268948408070425

Mol. Cryst. Liq. Cryst., 1984, Vol. 104, pp. 207–230
0026-8941/84/1044-0207/$18.50/0

Printed in the United States of America

Harmonic Dynamics of Anthracene Crystal

T. A. KRIVENKO†, V. A. DEMENTJEV‡, E. L. BOKHENKOV†,
A. I. KOLESNIKOV†, and E. F. SHEKA†

(*Received May 13, 1982; in final form September 13, 1983*)

A method is suggested for the calculation of the complete phonon spectrum of a polyatomic molecular crystal in the entire Brillouin zone. The spectrum includes both external and internal phonons and the method involves breaking up the high order dynamical matrix into several blocks covering large groups of phonons revealing marked intermode mixing inside a group and negligible mixing among the modes of the neighbouring groups. The phonon mode structure is assigned through the analysis of the eigenvector matrix. The calculations using the suggested method are controlled by the calculation of all 144 frequencies at the point $\mathbf{q} = 0$. The dispersion curves and the density of states of the entire 144-mode phonon spectrum of anthracene-d_0 crystal are presented.

1. INTRODUCTION

The harmonic lattice dynamics of molecular crystals has become a well-developed area for the last twenty years. This can be said about not only traditional aspects of low frequency external phonons but the complete phonon spectrum including both external and internal modes. Nevertheless, the computation of such a spectrum remains a complicated problem. So far only a few attempts have been made to compute a multimode spectrum.

On the other hand, these calculations are needed in connection with the new facilities of the neutron spectroscopy of phonons. The

†Institute of Solid State Physics of the Academy of Sciences of the USSR, 142432 Chernogolovka, USSR.
‡Timiryazev Agricultural Academy, 125008, Moscow, USSR.

high-flux-reactor experiments have shown that the phonon dispersion investigations of such classical species of molecular crystals as naphthalene,[1-3] benzene,[4] anthracene[5] and some others have ceased being only exotic and are becoming a practical spectroscopy. These measurements have been performed in a rather narrow energy region (0 − 200 cm^{-1}) and have covered only low frequency phonons. Despite the fact that the phonon dispersion could be successfully measured up to energies 700 cm^{-1},[6] there is scarce information concerning the internal phonon dispersion, based only on measurements of the density of states at an inelastic incoherent neutron scattering (IINS).[7-9] The progress in experimental investigations of the dispersion is partly restrained by the lack of dynamical structure factor calculations.

2. STATEMENT OF THE PROBLEM

The total number of phonon modes of a molecular crystal is $n = 3N\sigma$; N being the number of atoms in a molecule, σ is the number of molecules per unit cell. For benzene and anthracene $n = 144$, for naphthalene $n = 108$. The solution of the n-th order secular equation for all modes at an arbitrary point of the Brillouin zone (BZ) is a highly complicated problem and is not, practically, feasible even with the capabilities of modern computers. Therefore, approximations permitting reductions of n are used in realistic calculations.

A natural approximation, the so called rigid body approximation (RBA) separating phonon modes to the external and internal ones,[10] is based on the existence of an energy gap between them. In the RBA the external frequencies are found from the secular equation of the order $n = 6\sigma$. This approach in its most complete form was developed by Pawley.[11,12] His CRASH program was employed successfully to calculate the dispersion curves, eigenvectors and densities of states of external phonons in several crystals.[3,8,13-17]

To describe the internal phonons the vibrational exciton approximation (VEA) is generally used.[18,19] In the VEA each internal vibration is considered individually.

Pawley and Cyvin were the first to accomplish a precise solution of a complete multimode dynamical problem for naphthalene crystal.[20] It was made at selective points in the BZ where n is reduced by a factor of four or two due to symmetry.

A different approach to this problem was realized by Taddei *et al.* in the BENZ program[21] for benzene crystal. As in the previous case, the dynamical matrix is divided into 8 independent blocks at the BZ centre due to the number of irreducible representations of the factor

group. As contrasted from the method of Pawley and Cyvin this matrix does not contain the force constants of intramolecular interactions but, rather, the frequencies themselves and the derivatives of the intermolecular potential by the atom displacements in normal vibrations of the free molecule.

A comparison of the RBA with the precise calculations has shown that the former is good enough for naphthalene and benzene crystals.[1-3,8,9,16,20,21] Another situation occurred in anthracene: no gap exists between the external and internal modes in its phonon spectrum. Due to this fact, the RBA is too rough here. This situation is rather ordinary among complex aromatic molecules most of which possess low frequency vibrational modes.

Recently, several restricted solutions of this problem have been suggested.[22-24] In all the cases the solution reduces to an increase of the 6σ-th order of the dynamical matrix for the external phonons up to $(6 + k)\sigma$, where k is the number of the internal modes under consideration alongst the external ones. Although approximate result can be achieved with this formulation of the problem, the question of the validity of such an approach remains and the criteria imposed on the k value, at which the obtained solutions might be considered reliable enough, are still obscure. This problem together with the problem of the internal modes dynamics necessitates a search for calculations of the complete multimode spectrum of a molecular crystal at an arbitrary point of the BZ.

In this work we suggest a method for the computation of such a spectrum. It is based on breaking up a high order dynamical matrix into a small number of blocks covering groups of phonons thus enabling the calculation over the entire BZ. For the first time such calculations were performed for the 144-mode spectrum of anthracene. The BENZ program[21] was used in the calculation.

3. A DYNAMICAL MATRIX IN THE BENZ PROGRAM

When constructing a harmonic dynamical matrix the normal coordinates of individual molecule were used[21] under the assumption that the deformation of the equilibrium configuration of the free molecule is negligible in the crystal lattice. The elements of the dynamical matrix have the form

$$D_{\mu l}^{\eta m}(\mathbf{q}) = \sum_{\beta} \exp\{-i\mathbf{q}\mathbf{r}_{\beta}\} \left(\frac{\partial^2 V}{\partial Q_{1\mu l}\, \partial Q_{\beta\eta m}} \right). \qquad (1)$$

Here V is the intermolecular nonbonded pairwise atom-atom interaction potential in the analytical form "6-exp" with a set of phenomenological parameters. $Q_{\beta\eta m}$ is a normal coordinate for the m-th normal mode of the η-th molecule located in the β-th unit cell, $\mathbf{r}_\beta$ is the vector coupling the β-th unit cell with the coordinate origin. The phonon frequencies of the crystal, $\nu(\mathbf{q})$, are determined from the secular equation of order $3N\sigma$

$$|D_{\mu l}^{\eta m}(\mathbf{q}) + 4\pi^2\left[\nu_l^2 - \nu^2(\mathbf{q})\right]\delta_{lm}\delta_{\mu\eta}| = 0, \tag{2}$$

where ν_l is the l-th mode frequency of the free molecule.

This approach is easily simplified to cover approximate treatment such as the RBA (every $\nu_l = 0$) and the VEA for the internal modes ($\nu_l \neq 0$ for one l-th mode only).

The vibration frequencies and Cartesian displacements of the atoms of the free anthracene molecule needed to calculate the dynamical matrix elements were obtained in this work by the solution of the vibrational inverse spectral problem using the service computer program.[25] The atomic displacements are published separately in Ref. [26].

4. SYMMETRY PROPERTIES OF PHONONS IN ANTHRACENE CRYSTAL

Anthracene crystallizes in the monoclinic system, space group C_{2h}^5—$P2_1/a$, with two molecules per unit cell lying on sites of C_i

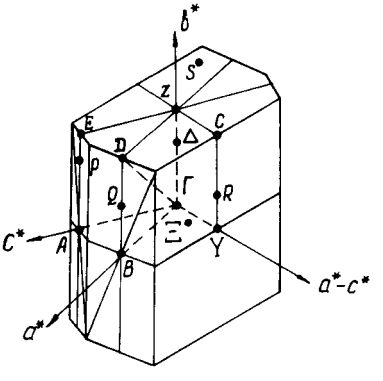

FIGURE 1 Brillouin zone of a monoclinic crystal.[28]

symmetry. The crystal structure is known at different temperatures.[27] 66 vibrations of the free molecule (its chemical formula is $C_{14}H_{10}$) are classified by the irreducible representations of the D_{2h} point group in the following way:

$$12A_g + 4B_{1g}^* + 6B_{2g}^* + 11B_{3g} + 5A_u^* + 11B_{1u} + 11B_{2u} + 6B_{3u}^*,$$

where the asterisk denotes the non-planar vibrations.

The BZ of the monoclinic crystal, showing the high symmetry points pertinent to the present calculations, is shown in Figure 1. Table I reports the characters of projective representations of the wave vector group according to Kovalev[29] for the high symmetry points, directions and planes of the BZ. The notation given by Zak *et al.*[28] is used for labeling the irreducible representations. The components of the q-vectors and the extra-degeneracy due to time reversal symmetry are also given in Table I.

As it is seen from the Table, the order of the secular equation can be reduced, for instance, by a factor of four at the points Γ, A, D and by two at the points Ξ, S, Δ, Q and so on.

5. THE q = 0 FREQUENCY SPECTRUM

Reducing the 144-th order secular equation at the Γ point by four the 36-th order equations enabled us to accomplish their precise numerical calculation. We used two sets of the parameters of the atom-atom potential and the structural data at $T = 5K$ (set II from [27]) that most closely correspond to the "harmonic" cell structure.†

Tables II and III report the calculational results. In the calculations all nonbonded interactions within a sphere, centered on each atom, with a radius of 5.5 Å were taken into account.

For convenience, the data obtained are classified into 72 factor-group (Davydov's) doublets: 36 for g- and 36 for u-modes. Of these, 66 doublets correspond to Davydov's splittings of 66 vibrations of the free molecule. Three low-frequency doublets in each Table correspond to the external degrees of freedom of the molecule in the crystal.

†The unit cell parameters were determined experimentally.[27] The atomic positions were obtained by minimization of the crystal potential energy at this fixed cell dimension.

TABLE I

Character of projective representations of the C_{2h}^5 group of monoclinic crystal.[29]

Point group	C_{2h}									C_h		C_2	
representations / symmetry elements	$\Gamma_1(A_1)$	$\Gamma_2(A_2)$	$\Gamma_3(A_3)$	$\Gamma_4(A_4)$	$Z(B,E)$	D_1	D_2	D_3	D_4	$\Xi_1(S_1)$	$\Xi_2(S_2)$	$\Delta_1(Q_1,P_1)$	$\Delta_2(Q_2,P_2)$
E	1	1	1	1	2	1	1	1	1	1	1	1	1
C_2	1	1	−1	−1	0	1	1	−1	−1			1	−1
i	1	−1	1	−1	0	1	−1	1	−1				
σ_h	1	−1	−1	1	0	−1	1	1	−1	1	−1		
High symmetry points and directions in BZ[a]	$\mathbf{q}=0\,(\Gamma)$;		$\mathbf{q}=\frac{\mathbf{c}^*}{2}(A)$		$\mathbf{q}=\frac{\mathbf{a}^*}{2}(B)$		$\textcircled{\mathbf{q}}=\frac{\mathbf{a}^*+\mathbf{b}^*}{2}(D)$			$\mathbf{q}=\xi_1\mathbf{a}^*+\xi_3\mathbf{c}^*(\Xi)$[c]		$\mathbf{q}=\xi_2\mathbf{b}^*$	(Δ)
					$\mathbf{q}^b=\frac{\mathbf{a}^*+\mathbf{c}^*}{2}$		$\textcircled{\mathbf{q}}^b=\frac{\mathbf{a}^*+\mathbf{b}^*+\mathbf{c}^*}{2}$			$\textcircled{\mathbf{q}}=\xi_1\mathbf{a}^*+\xi_3\mathbf{c}^*+\frac{\mathbf{b}^*}{2}(S)$		$\textcircled{\mathbf{q}}=\frac{\mathbf{a}^*}{2}+\xi_2\mathbf{b}^*$	(Q)
					$\mathbf{q}=\frac{\mathbf{b}^*+\mathbf{c}^*}{2}(E)$							$\textcircled{\mathbf{q}}^b=\frac{\mathbf{a}^*+\mathbf{c}^*}{2}+\xi_2\mathbf{b}^*$	
					$\mathbf{q}=\frac{\mathbf{b}^*}{2}(Z)$							$\mathbf{q}=\xi_2\mathbf{b}^*+\frac{\mathbf{c}^*}{2}$	(P)

[a] Circles label the wave vectors corresponding to twice degeneracy due to the time reversal symmetry.
[b] These vectors are equivalent to the vectors along the ΓZ axis (see Figure 1)
[c] $0 < \xi_i < 0.5$, where $i = 1, 2, 3$. Variables ξ_i describe the wave vectors in the Brillouin momentum units.

When calculating the crystal frequencies ν_{calc} we tried to fit them to the measured values by varying the initial input ν_l data. For a great majority of the internal phonons the fitting might be of any desired accuracy. Excluded are the cases of an occasional resonance of the modes. This situation takes place, for instance, for six modes related to the factor-group doublets NN 15 to 17 in the Table II. The change of ν_l by ~ 1 cm^{-1} does not only result in changes of the phonon frequencies by 10 cm^{-1} but, also, in a change of the phonon mode sequence. The assignment of "Davydov's doublets" for these modes is complicated.

The problem of shifting ν_l is somewhat inverse to that we usually meet when computing the free molecule frequencies.[25] The fact that these values themselves are not known experimentally but are obtained by calculations, is the reason for that. The corrected new set $\tilde{\nu}_l$ of the input data that produced the best fitting ν_{calc} to ν_{exp} are reported in the fourth columns of Tables II and III.

They are obtained using the Williams' set of parameters. As it is seen from the Tables the calculated results for high frequency external modes with these parameters fit better the experimental results than the data calculated with Kitaigorodsky' parameters. This fact was the reason for making all further calculations with Williams' parameters only. The calculated data ν_{calc} with Kitaigorodsky' parameters presented in Tables 2 and 3 show the influence of the potential parameters on the obtained results when the $\tilde{\nu}_l$ input data are fixed. When varying the ν_l values the Cartesian atomic displacements in normal vibrations remained fixed. A low sensitivity of the displacements to small changes of frequencies is well known.[20,41]

As seen from Tables II and III the values of the factor-group splitting are small for all internal modes (mode 40 excluded) in accordance with the fact that no such splittings were, practically, observed in the experimental spectra.

Tables II and III reveal pronounced shifts of the ν_{calc} data with the input $\tilde{\nu}_l$. These shifts are the well known static gas-crystal shifts in exciton theory.[42] They turned out to be larger for non-planar vibrations (on the average, 20 cm^{-1}) than for planar ones (~ 4 cm^{-1}). The obtained big shift values lead to the suggestion that the difference between the experimental frequencies of the free anthracene molecule and of the crystal should be observable. Actually, such a difference has been observed but for five low frequency vibrations of naphthalene.[43] The gas-crystal shift was found to be 11 and 26 cm^{-1} for the two factor-group components of the lowest non-planar B_{3u}^* mode and not to exceed 1–4 cm^{-1} for the other 4 planar modes, in

TABLE II

Calculated $\mathbf{q} = 0$ phonon frequencies of g-type of anthracene-d_0 crystal, cm^{-1}.

Doublet number	Mode symmetry in D_{2h}	ν_l calc. this work	$\tilde{\nu}_l$	ν_{exp}[a]	ν_{calc}[b]		Davydov's splitting	ν_{calc}[c]		Davydov's splitting
					A_g	B_g		A_g	B_g	
1		0	0	49/56[30]	50.1	57.7		56.6	60.9	
2		0	0	82/70[30]	88.2	76.4		96.4	83.9	
3		0	0	132/140[30]	145.6	147.8		173.2	162.4	
4	B_{1g}^*	244	217.6	247/244.5[31]	243.8	239.2	4.6	249.8	243.7	6.0
5	B_{2g}^*	113	248.7	290[32]	286.9	292.2	−5.4	299.2	308.2	−9.0
6	B_{3g}	362	384.9	390[32,33]	390.7	389.2	1.5	393.2	390.5	2.7
7	A_g	372	389.2	395[33]	396.2	393.8	2.4	399.1	395.7	3.4
8	B_{3g}	511	474.1	478.5/481[31]	475.0	474.2	0.8	475.5	475.0	0.5
9	B_{1g}^*	483	463.2	477[33]	478.7	476.5	2.2	483.2	479.9	3.3
10	B_{2g}^*	566	563.3	577[33]	575.9	578.0	−2.2	579.1	583.5	−4.4
11	A_g	642	617.0	622[33]	622.5	621.9	0.6	623.6	622.5	1.1
12	B_{1g}	743	725.0	747[33]	750.3	743.4	7.0	760.5	761.6	−1.1
13	A_g	743	746.4	753[32,33,34]	751.6	754.8	−3.1	752.8	747.9	4.9
14	B_{2g}^*	795	743.4	762.5/764[31]	765.0	765.4	−0.4	772.6	774.1	−1.6
15	B_{2g}^*	861	873.1	896[33]	886.8	889.6	−2.8	892.7	891.6	1.2
16	B_{1g}^*	942	893.8	904[32]	909.1	910.0	−0.9	919.8	924.2	−4.4

17	B_{2g}^{*}	911	872.9	918/916[31]	915.8	913.7	2.1	937.1	932.9	4.2
18	B_{3g}	923	954.0	954/959[31]	955.4	956.6	−1.1	957.0	958.4	−1.4
19	B_{2g}^{*}	986	957.8	980/978.5[31]	977.0	979.0	−2.1	986.8	990.2	−3.4
20	A_g	1019	1005.7	1008[32,33,34]	1008.3	1007.6	0.7	1009.2	1009.0	0.2
21	B_{3g}	1090	1097.7	1103[33]	1103.3	1102.6	0.7	1105.6	1104.9	0.7
22	A_g	1160	1151.5	1163[32,33,34]	1161.2	1164.8	−3.6	1165.7	1169.4	−3.7
23	B_{3g}	1217	1182.1	1187[33]	1186.5	1187.5	−1.0	1189.9	1191.8	−1.9
24	A_g	1234	1258.5	1261[32,33,34]	1261.6	1260.3	1.3	1263.4	1261.5	1.9
25	B_{3g}	1276	1271.2	1274[33]	1273.9	1274.0	−0.1	1276.6	1277.1	−0.5
26	B_{3g}	1403	1370.0	1376[33]	1376.3	1375.7	0.6	1379.4	1378.3	1.0
27	A_g	1384	1400.8	1403[32,33,34]	1403.2	1402.8	0.3	1404.3	1403.6	0.7
28	A_g	1460	1480.0	1482[33]	1482.6	1481.6	1.0	1483.8	1482.4	1.4
29	A_g	1600	1556.6	1557[33]	1557.0	1557.0	0.0	1557.0	1557.1	−0.1
30	B_{3g}	1563	1575.8	1576[33]	1576.0	1576.1	−0.1	1576.1	1576.2	−0.1
31	B_{3g}	1610	1633.7	1634[32,33,34]	1634.0	1633.9	0.1	1634.1	1634.0	0.1
32	B_{3g}	2986	2986.0		2987.8	2988.4	−0.6	2989.2	2990.1	−0.9
33	B_{3g}	3040	3040.0		3048.0	3047.4	0.6	3053.5	3053.3	0.2
34	A_g	3007	3060.1	3066[34]	3065.3	3066.7	−1.5	3070.2	3071.5	−1.3
35	A_g	3036	3084.7	3088[34]	3088.0	3088.0	0.0	3090.8	3090.7	0.0
36	A_g	3045	3101.0	3108[34]	3108.7	3107.3	1.3	3115.5	3113.5	2.0

[a]Experimental data correspond to 4.2K[30,31] and 293K.[32-34] Factor group components are established only for several doublets.
[b] and [c]Calculations were performed with Williams'[35] and Kitaigorodsky'[36] sets of parameters, respectively.

TABLE III

Calculated $\mathbf{q} = 0$ phonon frequencies of u-type of anthracene-d_0 crystal, cm^{-1}.

Doublet number	Mode symmetry in D_{2h}	ν_l calc. this work	$\tilde{\nu}_l$	ν_{exp}[a]	ν_{calc}[b]		Davydov's splitting	ν_{calc}[c]		Davydov's splitting
					A_u	B_u		A_u	B_u	
37		0	0	0/71.3[37]	0	59.7		0	65.4	
38		0	0		36.4	0		39.5	0	
39		0	0	107[37]/0	109.8	0		112.5	0	
40	B_{3u}^*	95	83.2	129/111[37]	126.8	111.0	15.8	131.4	114.4	17.0
41	A_u^*	179	74.6	172[37 d]	166.5	169.6	−3.1	186.9	190.7	−3.8
42	B_{1u}	221	227.4	235[38]	236.0	233.3	2.7	240.1	234.7	5.4
43	B_{3u}^*	350	463.3	475[39]	471.3	478.5	−7.3	472.7	481.9	−9.2
44	A_u^*	499	499.0		511.6	516.0	−4.4	515.8	521.0	−5.3
45	B_{3u}^*	496	589.6	603[39]	599.2	605.4	−6.1	605.1	611.5	−6.4
46	B_{2u}	593	596.5	600[38]	601.2	600.0	1.2	600.0	601.0	−1.0
47	B_{1u}	654	645.7	650[38]	650.4	649.6	0.8	652.4	650.7	1.7
48	B_{3u}^*	737	710.1	727[39,40]	730.6	723.4	7.2	735.5	730.9	4.6
49	A_u^*	783	783.0		788.0	788.4	−0.4	788.3	788.4	−0.2
50	B_{2u}	832	804.9	808[38]	808.9	807.2	1.7	810.2	808.1	2.1
51	A_u^*	853	841.7	870[40]	869.3	870.6	−1.2	880.5	880.4	0.1
52	B_{3u}^*	899	863.3	883[38,40]	883.9	882.4	1.5	896.0	892.9	3.1

53	B_{1u}	894	899.9	903[38]	903.0	903.0	0.1	904.9	904.1	0.8
54	B^*_{3u}	950	938.7	954[38,40]	953.5	954.5	−1.0	963.4	965.2	−1.8
55	A^*_u	968	968.0		989.8	991.9	−2.1	1003.5	1004.1	−0.6
56	B_{2u}	1007	995.7	998[38]	998.2	997.6	0.6	999.0	998.3	0.7
57	B_{2u}	1149	1063.0	1068[38]	1069.5	1071.5	−2.0	1074.3	1075.9	−1.5
58	B_{1u}	1131	1140.2	1145[38]	1144.7	1145.4	−0.7	1146.9	1148.7	−1.8
59	B_{2u}	1202	1160.1	1163[38]	1161.6	1164.5	−2.8	1162.8	1167.3	−4.5
60	B_{1u}	1254	1267.3	1270[38]	1269.3	1270.7	−1.4	1270.5	1273.2	−2.6
61	B_{1u}	1289	1310.8	1314[38]	1314.8	1313.2	1.6	1317.8	1314.7	3.1
62	B_{2u}	1307	1345.5	1346[39]	1346.2	1346.0	0.2	1346.7	1346.2	0.6
63	B_{2u}	1361	1397.0	1398[39]	1397.7	1398.4	−0.7	1398.1	1398.9	−0.8
64	B_{1u}	1425	1443.4	1447[38]	1447.0	1446.9	0.1	1448.8	1448.7	0.0
65	B_{2u}	1427	1459.5	1462[39]	1462.9	1461.2	1.7	1464.7	1462.3	2.5
66	B_{2u}	1542	1532.4	1533[39]	1533.0	1533.0	0.0	1533.1	1533.1	0.0
67	B_{1u}	1616	1615.7	1616[38]	1616.1	1616.0	0.1	1616.1	1616.1	0.0
68	B_{1u}	2986	3018.8	3024[38]	3023.7	3024.2	−0.5	3027.1	3027.9	−0.8
69	B_{2u}	3007	3047.0	3050[38]	3049.0	3051.0	−2.0	3051.1	3054.1	−3.0
70	B_{1u}	3036	3045.8	3050[38,40]	3050.0	3050.0	0.0	3052.8	3052.8	0.0
71	B_{2u}	3045	3086.8	3093[38]	3093.8	3092.1	1.8	3099.4	3096.3	3.1
72	B_{1u}	3040	3099.8	3108[38]	3108.4	3107.7	0.6	3116.1	3115.5	0.7

[a] Experimental data correspond to 4.2 K[37] and 296 K.[38–40] Assignment of the five lowest u-modes to symmetry types are performed in this work.
[b] and [c] Calculations were performed with Williams' [35] and Kitaigorodsky' [36] sets of parameters, respectively.
[d] For this mode and further ones no data are available on the factor group splitting.

TABLE IV

Calculated eigenvectors of A_g-phonons of anthracene-d_0 crystal at the Γ point.

Mode number	$\nu(q = 0)$	Mode number of g-basis of the free molecule																	
		1	2	3	4	5	6	7	8	9	10	11	12	13	14	15	16	17	18
	calc.	R_z	R_y	R_x	B^*_{1g}	B^*_{2g}	B_{3g}	A_g	B_{3g}	B^*_{1g}	B^*_{2g}	A_g	B^*_{1g}	A_g	B^*_{2g}	B^*_{2g}	B^*_{1g}	B^*_{2g}	B_{3g}
1	50.1	968	198	149	17	12	7	9	1	2		3	5	1	2		1	2	1
2	88.2	169	962	191	97	5	10	9	3	6	1		19	1	4	3	4	3	2
3	145.6	182	164	963	49	89		10	1	27	15	8	7	2	35	13	7	14	1
4	243.8	9	90	61	993	35	11	20	2	2	2	4	22	1	6	6	14	4	1
5	286.9	7	18	89	32	992	56	6	15	3	35	12	5	3	13	20	2	27	1
6	390.7	8	10	6	15	53	924	372	3	59	7	5	13	2	1	6		4	1
7	396.2	6	8	10	16	16	371	928	20	19	6	1	4	3	4	4	6	1	
8	474.9		1	9	3	12	7	18	955	294	7	8	7	1	6	1	3	6	1
9	478.7	3	11	22	2	6	62	1	294	952	30	16	23	2	11	9	17	3	4
10	575.9	3	2	11		35	5	3	14	26	997	30	11	1	20	28	3	29	3
11	622.5	4		8	4	12	5	3	3	16	30	999		6	4	1	8	6	1
12	750.3	1	20	1	18	3	9	8	1	21	5	3	898	421	118		12	26	11
13	751.6	1	9	1	9	4	7	1	1	7	4	6	414	906	82	12	6	2	
14	765.0	4	5	33	1	8		4	2	14	21	3	142	24	982	42	32	80	
15	886.8	1	1	19	4	1	4	3	1	3	3	3	6	1	72	761	184	614	10
16	909.1	1	2	14	11	26	5	3	5	7	26	8	15	11	57	360	676	636	26
17	915.8	2	4	4	10	24	2	4	6	17	28	4	2	10	6	532	709	453	60
18	955.4	1	2		1	3	1		1	5	5	1	9	5	4	33	26	50	997
19	977.0	4	5	23	1	6		2		8	16	2	19	6	63	58	55	45	24
20	1008.3	1		3	1		3			1	2	1	10		9	8	5	6	8
21	1103.3	2	1	3	2	1	5		1	1	4	1	5	1	3	13	1	5	
22	1161.2		6	1	7	1	2	4	2	1	3	2	19	5	1	7	19	7	4
23	1186.5		2	5	1	1	2	2	1	6			7		11	6	9	13	5
24	1261.6	1	1	4	1			2		4	1	4	2	3	5	8	5	2	1
25	1273.9	1	1	1	2	7	3	1	1	3	4	2	4	2		14	2	12	1
26	1376.3	3		2	1	1	3			1	1	1	3	2	2	3	1	1	1
27	1403.2		1	1	2		1	2	1	1	1	1	3	2	1	1	5	1	1
28	1482.6			1	1	1	2	2						2	2	3	3		
29	1557.0				1					1			1	1		1	1		1
30	1576.0																		
31	1634.0																1	1	
32	2987.8												1						
33	3048.0		1	1		1	1			1	1		2		1	1	1	1	
34	3065.3	1			1			1					1				2		
35	3088.0					1												1	
36	3108.7			1				1		1		1	1	1	1	1	1		

TABLE IV *Continued*

Mode number	$\nu(\mathbf{q}=0)$	Mode number of g-basis of the free molecule																	
		19	20	21	22	23	24	25	26	27	28	29	30	31	32	33	34	35	36
	calc.	$B_{2g}^{\star}$	A_g	B_{3g}	A_g	B_{3g}	A_g	B_{3g}	B_{3g}	A_g	A_g	A_g	B_{3g}	B_{3g}	B_{3g}	B_{3g}	A_g	A_g	A_g
1	50.1		1	3	1				2								1		
2	88.2	2	1		4	3	1	1		1									
3	145.6	18	2	2	1	3	3		2	1	1					1			1
4	243.8		1	2	7	1	1	2	1	1	1	1					1		
5	286.9	8		1		1	1	6								1		1	
6	390.7	1	3	5	1	1		2	3		1					1			
7	396.2	2	1	2	5	2	2	2	1	3	2					1	1		1
8	474.9	2		1	1		1	1		1									
9	478.7	5	1	1	2	6	3	3	1	1		1				1			1
10	575.9	15	1	3	3		1	4	1							1			
11	622.5	1	1	1	2		4	2	1	1									1
12	750.3	8	10	3	19	9	1	3	3	4	1				1	1	1		1
13	751.6	9	5	3	3	4	4	3	3	1	2	1				1	1		1
14	765.0	60	4	3	3	8	4		1	2	2					1			1
15	886.8	68	8	6	6	15	6	4	2	1	3			1					1
16	909.1	49	5	7	17	1	2	15	1	4	3						1	1	1
17	915.8	49	4	9	15	8	7	12	2	2	1	1		1		2	2	1	2
18	955.4	24	10		3	6	2		1	1		1				1			
19	977.0	991	53	11	14	12	6	1	4	2	2		1			2			
20	1008.3	53	998	16	5	3	2	3	4	1	3								
21	1103.3	10	16	999	23	4	1	1	17	2	2		1	1		1	1		
22	1161.2	14	4	23	998	48	7	5	7	15	9	1		1	1	1	2		1
23	1186.5	12	3	3	48	998	8	11	2	5	3	1		1		1	1		
24	1261.6	5	2	1	7	7	10^3	3	8	11	7	2	1						2
25	1273.9	1	3	1	6	10	3	10^3	4	4	6			1		1		1	
26	1376.3	4	4	17	7	2	7	4	999	33	7	2	4	1		1	1		
27	1403.2	3	2	3	15	4	11	4	32	999	27		1	1	1	1	1		1
28	1482.6	2	3	2	10	3	7	6	7	26	10^3	1	3	1		1	1		1
29	1557.0				1		2		2		1	10^3	1						
30	1576.0	1		1			1		4	1	3	1	10^3	3					
31	1634.0			1	1	1		1	1	1	1		3	10^3					
32	2987.8				1					1					10^3	8	18		20
33	3048.0	2		1	1	1		1	1		1				10	991	134		20
34	3065.3			1	2	1			1	1	1				17	134	991	2	14
35	3088.0							1								1	2	10^3	2
36	3108.7				1		2			1	1				20	21	12	2	999

agreement with the above. To make sure that this fact is not only an occasional coincidence we have carried out calculations for naphthalene[44] similar to those made for anthracene. A good agreement of the $\tilde{\nu}_l$ calculated data with the experimental free molecule frequencies[43] was obtained in this case. This fact makes us suggest that the $\tilde{\nu}_l$ set in Tables II and III describes the anthracene molecules vibrational spectrum rather well.

6. THE ANALYSIS OF A PHONON MODE STRUCTURE AND BREAKING UP OF THE DYNAMICAL MATRIX INTO BLOCKS

A realistic approach to the calculation of the phonon dispersion and the density of states is suggested by the form of the eigenvector matrix. Table IV represents one of four blocks, namely the block for 36 phonons of the A_g-factor-group symmetry, into which the full eigenvector matrix is divided at the Γ point. The eigenvector components are given without sign and scaled by 10^3 times. Vacant places correspond to the values lower than 1 in this scale. The value of the eigenvector component determines the contribution of the appropriate free molecule coordinate to the given phonon mode. Table IV actually reports the intermode mixing.

It is seen from Table IV that the dominant components with values of the order 10 and larger concentrate close to the diagonal. They can be grouped in 7 blocks. The blocks are shown by squares in Table IV. While grouping the main attention was paid to the dominant intermode mixing and to the energy intervals between neighbouring modes of the adjacent blocks. As it is seen from Table IV these intervals are of a hundred and more cm^{-1} whereas they are of unity and tens cm^{-1} within the blocks.

The same procedure was applied to the remaining three matrices for B_g-, A_u- and B_u-modes that were also broken up in seven blocks each. The joint matrix was constructed as consisting of seven joint blocks. Each of these joint blocks contains four blocks from the A_g-, B_g-, A_u- and B_u-matrices.

The block characteristics and the accuracy of the "block method" are given in Table V. The energy intervals between the edge frequencies of the adjacent joint blocks are sometimes smaller (tens cm^{-1}) than within the separate factor group matrices. But these intervals are formed by the modes of different symmetry that are not mixed at the

TABLE V

Block characteristics and the block method accuracy at the Γ point.

Block number	Number of modes	Mode composition in factor group components	Energy region, cm^{-1}	$\sum_{block} \lvert \nu_{prec} - \nu_{block} \rvert$, cm^{-1}	$R(\%)$
1	22	$5A_g + 5B_g + 6A_u + 6B_u$	0–300	38,2	1,3
2	20	$6A_g + 6B_g + 4A_u + 4B_u$	390–620	13,1	0,1
3	14	$3A_g + 3B_g + 4A_u + 4B_u$	650–810	5,4	0,05
4	24	$6A_g + 6B_g + 6A_u + 6B_u$	870–1010	20,9	0,1
5	18	$5A_g + 5B_g + 4A_u + 4B_u$	1070–1270	1,5	0,007
6	26	$6A_g + 6B_g + 7A_u + 7B_u$	1310–1640	1,1	0,003
7	20	$5A_g + 5B_g + 5A_u + 5B_u$	2980–3110	0,4	0,0007
Sum over all blocks	144		0–3110	80,6	0,05

Γ-point. As it will be shown later, this mode mixing has a negligible influence on the crystal frequency calculation at an arbitrary point of the BZ as well.

The accuracy parameter R is given as

$$R = \frac{\sum_{block} \lvert \nu_{prec} - \nu_{block} \rvert}{\sum_{block} \nu_{prec}} \cdot 100\%. \tag{3}$$

As seen from Table V, the results of the block calculations agree well with the precise calculation. The difference ~ 1% is only observed for the low frequency modes comprising the 1-st block. Qualitatively, this can be explained by a one-side location of the split-off modes, while for every internal block the pressure of these modes on both sides is compensated.

Table VI presents the $\mathbf{q} = 0$ frequencies involved in the 1-st block, calculated in the RBA, in the block and precisely. Table VI reports as well the experimental data. The assignment of the u-modes to the symmetry type is done in the present work.

As evidenced by Table VI, the block calculation somewhat overestimates the frequency values (~ 1 cm^{-1}) as compared with the exact calculations. Only for the six underlined modes is the discrepancy as large as 3 to 5 cm^{-1}. The analysis of the complete eigenvector matrix shows that for these modes there are some eigenvector components with values of the order of 10 outside the separated block in the

TABLE VI

Calculated $\mathbf{q} = 0$ phonon frequencies of anthracene-d_0 crystal covered by the first block, cm^{-1}.

Factor symmetry	ν_{RBA}	ν_{block}	$\nu_{prec.}$	$\nu_{exp.}$
	0	0	0	
	43.5	36.6	36.4	
	116.9	111.3	109.8	107[37]
A_u		127.7	126.8	129[37]
		171.3	166.5	172[37]
		236.3	236.0	235[38]
	62.6	60.8	59.7	71.3[37]
	0	0	0	
	0	0	0	
B_u		111.8	111.0	111[37]
		174.4	169.6	172[37]
		233.6	233.3	235[38]
	51.1	50.9	50.1	49[30]
	93.1	90.0	88.2	82[30]
A_g	153.9	151.7	145.6	132[30]
		245.1	243.8	247[31]
		289.9	286.9	290[32]
	59.3	58.4	57.7	56[30]
	78.4	78.0	76.4	70[30]
B_g	153.2	152.1	147.8	140[30]
		240.1	239.2	244.5[31]
		295.2	292.2	290[32]

energy region up to 1000 cm^{-1}. Actually, these deviations show a maximal error of the block calculation.

The effect of the external modes softening in going from the RBA to the block or precise calculations is also apparent from Table VI. An agreement between the calculated data and the experimental ones can be characterized by the parameter R by analogy with (3), if ν_{prec} and ν_{block} are replaced for ν_{exp} and ν_{calc}, correspondingly, where ν_{calc} are ν_{RBA}, ν_{block} and ν_{prec} from Table VI, respectively. Thus, for the external modes $R_{RBA} = 11.1\%$, $R_{block} = 9.3\%$ and $R_{prec} = 7.2\%$.

Grouping of the phonon modes based on the combined analysis of the energy intervals and eigenvector mode structure has been performed only at one point of the BZ. The effect of the block choice on the dispersion curves was checked by calculating a 30-modes block that joined the modes of the 2-nd and the 3-rd blocks (a part of the joint block is shown by the dashed square in Table IV). The calculation was done in five directions in the BZ. A comparison of the results for individual blocks and for joint ones showed excellent agreement: the frequency variations do not exceed 0.8 cm^{-1} throughout

the considered part of the BZ. We have chosen just the modes from the 2-nd and the 3-rd blocks for such a test due to the smallest (27 cm^{-1}) energy distance between them. This allows one to suggest that the set of blocks selected in the BZ center can be used over the entire BZ.

The correctness of the block separation can be checked for any individual case by calculating a test joint block combining the modes within the energy interval up to several hundreds cm^{-1}.

In the determination of the optimal block sizes the facility of the CDC-6600 or the BESM-6 computers was taken into account. The maximum block, which can be placed in storage capacity, consists of 36 modes. But it takes an unrealistic long time to calculate the density of states in this case because the calculation time increases in proportion to the square of the number of modes. For instance the calculation of the density of states for 22 modes at 1800 points of the irreducible part of the BZ takes 9 hours. For practical calculations blocks containing from 14 to 26 modes were chosen (see Table V).

7. THE PHONON DISPERSION AND THE DENSITY OF STATES

The dispersion curves of all the phonon modes for anthracene $-d_0$ crystal were calculated in five directions of the BZ. The results are shown in Figures 2(a) to (f). Solid lines in the Figures designate the modes symmetric with respect to a two-fold axis (direction $\Gamma \rightarrow Z$) or to a glide plane (directions $\Gamma \rightarrow B$ and $\Gamma \rightarrow A$). Dashed lines in these directions correspond to antisymmetric modes. The small step calculations ($\Delta\xi = 0.005$) performed at several points of the BZ enabled one to establish the existence of finite energy gaps between the nearest branches of the same symmetry, i.e. the anticrossing effect.

The phonon density of states normalized to unity ($\int g(\nu)\, d\nu = 1$) was calculated by a 1 cm^{-1} step histogram technique in 6859 points of the BZ and is presented in Figure 3. For branches with a small dispersion the number of points in the BZ was decreased (minimum number was 343).

The 0-200 cm^{-1} low frequency region (Figure 2a) contains 16 branches. They all have pronounced dispersion. Of these, 12 branches originated from the displacements of the molecules as a whole and 4 branches correspond to two internal normal coordinates of B_{3u} and A_u symmetry of the free molecule. In Figure 2a, the density of states in this region ① covers a wide range. For comparison, the similar figure

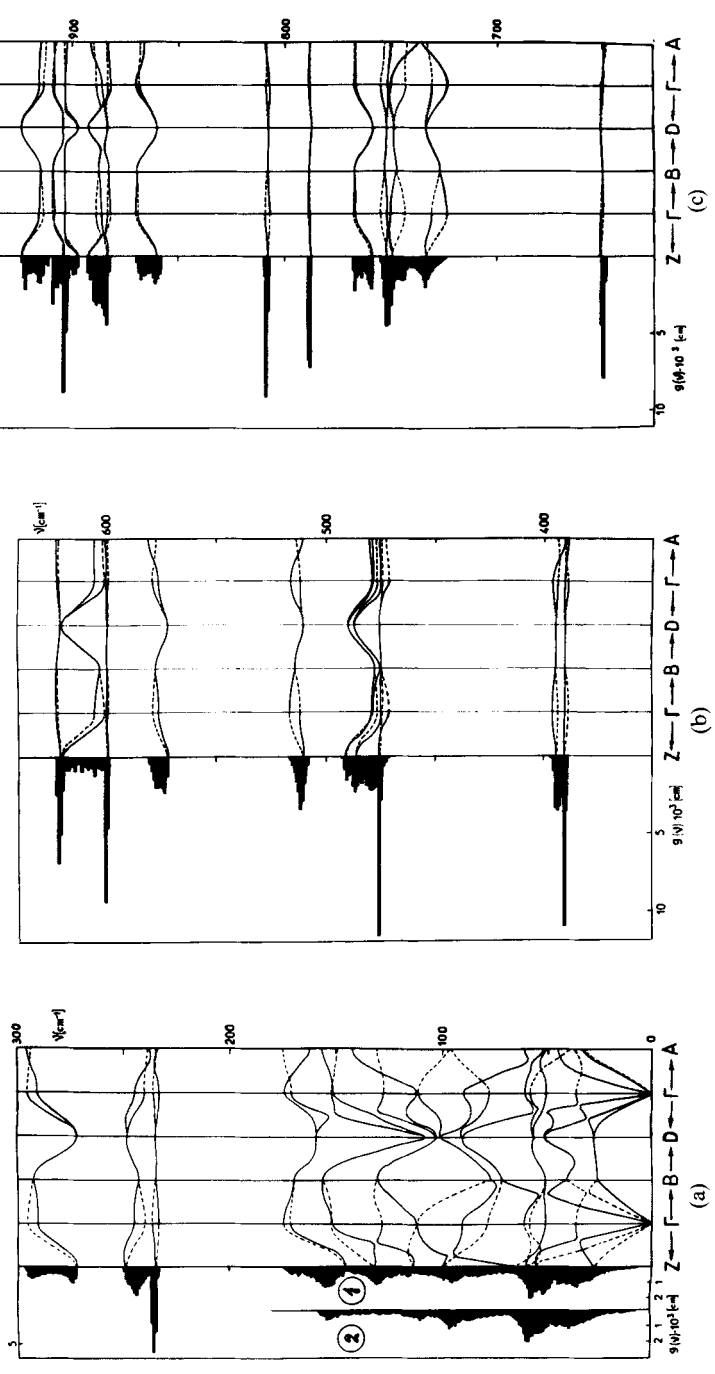

FIGURE 2 Block calculated harmonic dispersion curves and densities of states of anthracene-d_0 crystal. (a) 1-st block; (b) 2-nd block; (c) 3-rd and 4-th blocks; (d) 5-th block; (e) 6-th block; (f) 7-th block. For the block description see Table 5.

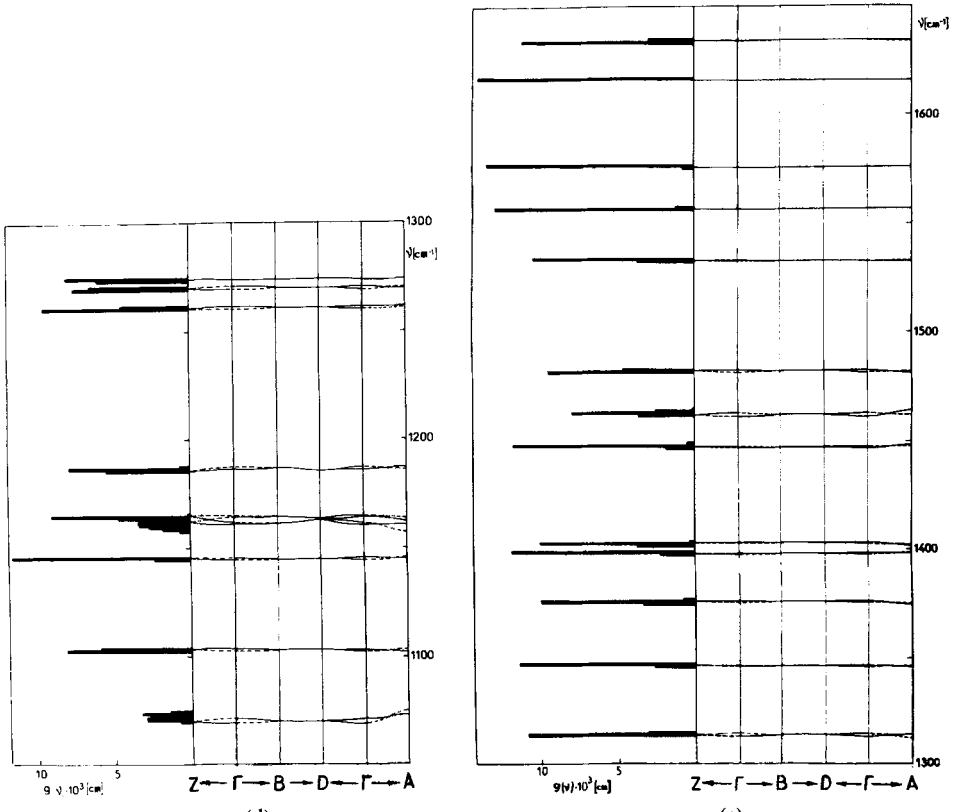

(d) (e) (f)

FIGURE 2 *Continued*

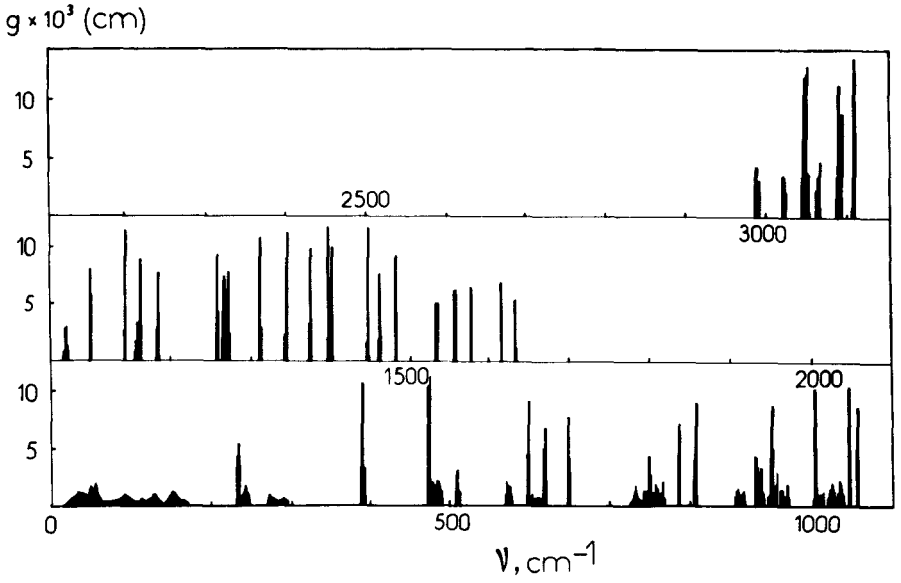

FIGURE 3 Harmonic density of states of the 144-mode phonon spectrum of anthracene-d_0 crystal.

presents the density of states ② calculated in the RBA. The inclusion of the internal modes is seen to reconstruct the density of phonon states markedly.

In the 100–200 cm^{-1} range the external modes become strongly mixed with two internal ones. The effect of this mixing on the dispersion curves is illustrated in Figure 4. Figure 4a demonstrates the dispersion curves for the internal modes 1 and 3 calculated for each mode independently in the VEA;† the RBA was used for the external mode 2. The curves presented in Figure 4b are obtained for these internal modes in the VEA as well but with the intermode mixing. The calculation of these three curves inside the 1-st block gives in this region a pattern shown in Figure 4c. Due to the strong intermode mixing the dispersion curves become repulsed and transformed. The character of the motions in these branches varies strongly over the BZ as illustrated in Table VII, where the changes of the eigenvector mode structure are shown for the direction $\Gamma \rightarrow Z$. Thus, branch 2 at the BZ

†The VEA implies the calculation in the basis containing one (the case in Figure 4a) or two (the case of Figure 4b) intramolecular modes.

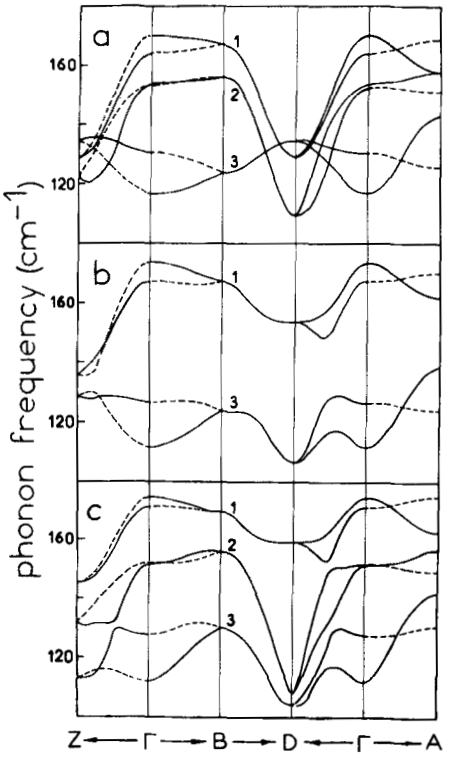

FIGURE 4 Dispersion curves of anthracene-d_0 crystal in the 110–170 cm^{-1} region. (a) 1 and 3 are calculations of the A_u and B_{3u} internal modes independently in the VEA; 2-separate calculation of the external R_x mode in the RBA; (b) 1 and 3 are joint calculations of the A_u and B_{3u} internal modes in the VEA. (c) 1, 2 and 3-block calculation (see the text).

center has the character of an external rotational motion (the biggest component of the eigenvector is $R_x = 0.682$) but at the point (0, 0.5, 0) it exhibits the internal mode of A_u symmetry. A noticeable mixing is observed in other spectrum regions, too.

It should be pointed out that many phonon modes have a small factor-group splitting at the Γ point and a considerable dispersion over the BZ. For instance, the mode with $\tilde{\nu}_5 = 248.7$ cm^{-1} has the splitting 5.4 cm^{-1} (doublet 5 in Table II), while the band width for this mode equals 24 cm^{-1}. The same is the mode behaviour for Davydov's doublets 8, 9 and 45 (Tables II and III) in Figure 2b and several others in Figure 2c. This fact disagrees with the common opinion of low dispersion for the modes which demonstrate small Davydov's splittings in optical spectra.

TABLE VII

Mode structure of eigenvectors for six dispersion branches from block 1 in the $\Gamma \rightarrow Z$ direction of the BZ.[a]

Doublet[b] number	ξ	Symmetry	ν, cm^{-1}	T_x	T_y	T_z	R_x	R_y	R_z	A_u^*	B_{3u}^*	B_{1u}	B_{1g}^*	B_{2g}^*
41	0	A_u	171,3	48	72	−185	0	0	0	639	−214	62	0	0
(branch		B_u	174,4	8	−57	−24	0	0	0	680	−182	−9	0	0
1 in	1/6	A	164,6	45	65	−207	−116i	−73i	25i	601	−252	40	61i	−39i
Figure 3c)		B	167,2	−19	−72	−55	−133i	108i	−11i	−645	−208	5	−50i	−16i
	1/3	A	150,3	44	39	−257	−50i	−104i	−23i	469	−435	1	70i	−44i
		B	152,2	−43	−117	−195	−301i	165i	40i	−433	−368	25	−53i	−28i
	1/2		145,4	1	3	290	188	−96	−109	−82	588	−14	49	2
3	0	A_g	151,7	0	0	0	682	−115	−125	0	0	0	40	68
(branch		B_g	152,1	0	0	0	701	58	39	0	0	0	−44	−42
2 in	1/6	A	140,2	−30i	−68i	6i	664	154	−129	−86i	38i	−8i	40	51
Figure 3c)		B	148,8	−33i	−79i	−194i	621	−27	6	206i	138i	15i	40	39
	1/3	A	131,4	−17i	−72i	13i	−160	−2	144	448i	496i	5i	29	−1
		B	141,0	−10i	−49i	−247i	−307	−82	95	520i	−235i	6i	−28	−17
	1/2		131,8	−10	82	52	110	117	21	676	55	−13	31	−17
40	0	A_u	127,7	−96	10	8	0	0	0	227	662	27	0	0
(branch		B_u	111,8	−4	−26	−11	0	0	0	185	−682	−4	0	0
3 in	1/6	A	129,2	−74	32	18	9i	−25i	82i	271	641	23	15i	18i
Figure 3c)		B	113,9	−21	−9	−49	−189i	35i	−85i	−159	654	5	5i	15i
	1/3	A	116,5	37	−39	261	−536i	291i	79i	−1	−178	−8	−18i	−18i
		B	116,0	−72	−68	−234	362i	−48i	81i	−66	540	9	3i	14i
	1/2		113,0	94	−15	428	−367	202	−41	−35	−359	−8	−19	9

[a] The eigenvector components are increased by 10^3 times.
[b] Doublets are numbered in accordance with Tables II and III.

8. CONCLUSION

Calculation of the complete harmonic phonon spectrum of anthracene crystal over the entire BZ became realistic because of the breaking up of a high order dynamical matrix into several blocks. Each block involves large groups of phonons whose eigenvector mode structure is based on a similar restricted normal coordinate basis. This approach turned out to be rather successful. The calculated dispersion curves of the crystal are in good qualitative agreement with the experimental investigations of low temperature dispersion of phonon modes of anthracene-d_{10} crystal in the range 0–200 cm^{-1}.[5] Apart from the density of states shown in Figure 3 it turned out to be possible to calculate the density weighted by squared amplitudes of hydrogen atom displacements in anthracene-d_0 crystal. These calculational results fit well the experimental spectra of IINS from this crystal at low temperature for both the low-[45] and high[46] frequency phonon regions.

A physical substantiation to the procedure to use the reduced bases is the mode structure inhomogeneity of the multimode spectrum. This inhomogeneity is likely to take place in the phonon spectrum of any complex crystal, therefore the method suggested can be extended with confidence to other crystals.

Acknowledgments

The authors wish to express their deep gratitude to Prof. S. Califano and Dr. R. Righini for the fruitful discussions and for making the BENZ program available, to Dr. I. Natkaniec, Mrs. E. M. Rodina and Mr. A. V. Belushkin for help in the computational process. We thank Miss L. S. Krupskaya for the help in preparing the English version of the manuscript.

References

1. E. L. Bokhenkov, E. F. Sheka, B. Dorner and I. Natkaniec. *Solid St. Commun.*, **23**, 89 (1977).
2. G. A. Mackenzie, G. S. Pawley and O. W. Dietrich. J. Phys. C: *Solid St. Phys.*, **10**, 3723 (1977).
3. I. Natkaniec, E. L. Bokhenkov, B. Dorner, J. Kalus, G. A. Mackenzie, G. S. Pawley, U. Schmelzer and E. F. Sheka. *J. Phys. C: Solid St. Phys.*, **13**, 4265 (1980).
4. B. M. Powell, G. Dolling and H. Bonadeo. *J. Chem. Phys.*, **69**, 2428 (1978).
5. B. Dorner, E. L. Bokhenkov, S. L. Chaplot, J. Kalus, I. Natkaniec, G. S. Pawley, U. Schmelzer and E. F. Sheka. *J. Phys. C: Solid St. Phys.*, **15**, 2353 (1982).
6. P. Vorderwisch, S. Hautecler, R. Sherm and B. Dorner. Annex to the ILL Annual Report, 69 (1978).
7. E. L. Bokhenkov, I. Natkaniec and E. F. Sheka. *Phys. St. Sol. (b)*, **75**, 105 (1976).
8. E. L. Bokhenkov, I. Natkaniec and E. F. Sheka. *Sov. Phys.-JETP*, **43**, 536 (1976).

9. E. L. Bokhenkov, V. G. Fedotov, E. F. Sheka, I. Natkaniec, M. Sudnik-Hrynkiewicz, S. Califano and R. Righini. *Nuovo Cimento*, **44B**, 324 (1978).
10. G. Venkataraman and V. G. Sahni. *Rev. Mod. Phys.*, **42**, 409 (1970).
11. G. S. Pawley. *Phys. St. Sol.*, **20**, 347 (1967).
12. G. S. Pawley. *Phys. St. Sol.*, **49**, 475 (1972).
13. G. Dolling, G. S. Pawley and B. M. Powell. *Proc. Roy. Soc. London*, **A333**, 363 (1973).
14. R. P. Rinaldi and G. S. Pawley. *J. Phys. C: Solid St. Phys.*, **8**, 599 (1975).
15. C. G. Windsor, D. H. Saunderson, J. N. Sherwood, D. Taylor and G. S. Pawley. *J. Phys. C: Solid St. Phys.*, **11**, 1741 (1978).
16. E. L. Bokhenkov, I. Natkaniec and E. F. Sheka. *Phys. St. Sol. (b)*, **85**, 331 (1978).
17. G. S. Pawley, G. A. Mackenzie, E. L. Bokhenkov, E. F. Sheka, B. Dorner, J. Kalus, U. Schmelzer and I. Natkaniec. *Molec. Phys.*, **39**, 251 (1980).
18. N. Rich and D. A. Dows. *Molec. Cryst.*, **5**, 111 (1968).
19. J. C. Laufer and R. Kopelman. *J. Chem. Phys.*, **53**, 3674 (1970).
20. G. S. Pawley and S. J. Cyvin. *J. Chem. Phys.*, **52**, 4073 (1970).
21. G. Taddei, H. Bonadeo, M. P. Marzocchi and S. Califano. *J. Chem. Phys.*, **58**, 966 (1973).
22. E. Burgos, H. Bonadeo and E. D'Alessio. *J. Chem. Phys.*, **65**, 2460 (1976).
23. I. Natkaniec, A. V. Bielushkin and T. Wasiutynski. *Phys. St. Sol. (b)*, **105**, 413 (1981).
24. S. L. Chaplot, G. S. Pawley, B. Dorner, V. K. Jindal, J. Kalus and I. Natkaniec. *Phys. St. Sol. (b)*, **110**, 445 (1982).
25. V. A. Dementjev, V. I. Smirnov and L. A. Gribov. FORTRAN Programs for the Calculation of the Molecular Vibrations, VINITI, No. 4018/76; Ref. *Zhurn. Khim.*, 5B59, (1977).
26. T. A. Krivenko, V. A. Dementjev, E. L. Bokhenkov, A. I. Kolesnikov and E. F. Sheka. Preprint ISSPh, Chernogolovka (1982).
27. E. L. Bokhenkov, A. I. Kolesnikov, J. Majer and V. G. Fedotov. *Sov. Phys.—Crystallogr.* (1983) will be published.
28. J. Zak, A. Gasher, M. Glück and Y. Gur. The Irreducible Representations of Space Groups, New York: Benjamin (1969).
29. O. V. Kovalev. Irreducible Representations of Space Groups, Kiev, Ac. of Sci. (1961); Gordon & Breach (1965).
30. M. Ito, M. Suzuki and T. Yokoyama. in Excitons, Magnons and Phonons in Molecular Crystals, Beirut, Lebanon, The University Press, Cambridge 1968.
31. F. Z. Khellady. *Chem. Phys. Lett.*, **34**, 490 (1975).
32. M. Suzuki, T. Yokoyama and M. Ito. *Sp. Acta.*, **24A**, 1091 (1968).
33. J. Rasanen, F. Stenman and Penttonen. *Sp. Acta*, **29A**, 395 (1973).
34. N. Abasbegovic, N. Vacotuc and I. Colombo. *J. Chem. Phys.*, **41**, 2575 (1964).
35. D. E. Williams. *J. Chem. Phys.*, **45**, 3770 (1966); ibid **47**, 4680 (1967).
36. A. I. Kitaigorodsky. *J. Chim. Phys.* **63**, 9 (1966).
37. M. Hineno and H. Yoshinaga. *Sp. Acta*, **31A**, 617 (1975).
38. A. Bree and R. A. Kydd. *J. Chem. Phys.*, **48**, 5319 (1968).
39. S. Califano. *J. Chem. Phys.*, **36**, 903, (1962).
40. L. Colombo. *Sp. Acta*, **20**, 547 (1964).
41. G. Hagen and S. J. Cyvin. *J. Phys. Chem.*, **72**, 1446, 1451 (1968).
42. A. S. Davydov. Theory of Molecular Excitons, Moscow (1968).
43. J. A. Duckett, T. L. Smithson and H. P. Weiser. *J. Mol. Struct.*, **44**, 97 (1978).
44. A. I. Kolesnikov, T. A. Krivenko, E. L. Bokhenkov, V. A. Dementjev, and E. F. Sheka. *Fiz. Tverdogo Tela*, **25**, No. 10, 2881 (1983).
45. E. L. Bokhenkov, A. I. Kolesnikov, J. Maier, I. Natkaniec, V. G. Vedotov, E. F. Sheka. *Fiz. Tverdogo Tela*, **25**, 2264 (1983).
46. E. L. Bokhenkov, A. I. Kolesnikov, T. A. Krivenko, E. F. Sheka, V. A. Dementjev and I. Natkaniec. *J. de Physique*, **42**, C6-605 (1981).